

# IMAGE SEGMENTATION AS REGULARIZED CLUSTERING: A FULLY GLOBAL CURVE EVOLUTION METHOD

Carlos Vázquez, Amar Mitiche, and Ismail Ben Ayed

INRS-EMT, Institut National de la Recherche Scientifique  
Place Bonaventure, 800 de la Gauchetière West, Suite 6900  
Montreal QC, H5A 1C6, Canada

e-mail: [vazquez,mitiche,benayedi]@inrs-emt.quebec.ca

## ABSTRACT

The purpose of this study is to investigate image segmentation from the viewpoint of image data regularized clustering. From this viewpoint, segmentation into a fixed but arbitrary number  $N$  of regions is stated as the simultaneous minimization of  $N - 1$  energy functionals, each involving a single region and its complement. The resulting Euler-Lagrange curve evolution equations yield a partition at convergence provided the curves are initialized so as to define an arbitrary partition of the image domain. The method is implemented via level sets, and results are shown on synthetic and natural vectorial images.

## 1. INTRODUCTION

Image segmentation is a fundamental problem in digital image processing and computer vision. The introduction of active contours and level-sets brought forth a new class of tractable algorithms which have succeeded in segmenting difficult images. Active contour methods map regions to the interior of simple closed planar curves which evolve to segment the image. The two-region segmentation problem is rather straightforward to state. However, two-region algorithms are difficult to generalize to an arbitrary, albeit fixed, number of regions. The difficulty comes mainly from the fact that while a simple closed curve unambiguously defines a partition of the image domain, the interior and the exterior of the curve, two or more curves can intersect, causing regions they define to overlap and, therefore, ambiguity in segmentation.

The classic study of Zhu and Yuille [1] has firmly established the capability of curve evolution methods in image segmentation. In their method, each curve segment between two regions of an initial partition of the image domain is made to evolve according to a region competition strategy that preserves a partition of the image domain at all times. The method does not accommodate the level-set framework, and thus lacks the numerical stability and topology independence that level-sets afford. Also, a good initialization seems critical to a successful completion of the algorithm.

An alternative approach is to use several curves, the interior of each corresponding to a region of segmentation [2] [3] [4] [5]. In [2], Yezzi *et al.* use what they call a fully global functional to maximally separate the characteristics of the different regions of segmentation. This method yields a partition at convergence. Its

extension to more than two regions, however, is quite complex because it calls for the maximization of the volume of a polyhedron with as many vertices as regions. Another difficulty is that segmentation in  $N$  regions requires an  $N - 1$ -dimensional image function. In [3] Chan and Vese introduce what they refer to as multi-phase active contours. The method seeks a segmentation into up to a power of 2 number of regions. There is no clear indication on the actual number of regions the method yields since this depends not just on the image but also on the weight of the regularization term. In some instances, unwanted division of regions can occur, as with image segments of planar intensity variation.

Paragios and Deriche [4] and Samson *et al.* [5] use a weighed penalty term in the objective functional to penalize overlapping regions. If the weight of this partition term is too large, curve evolution is driven predominantly by this term and image data can be practically disregarded. On the other hand, if the weight is too small, overlapping can subside at convergence. It is not quite clear how to set the weight of this partition term.

In this study, image segmentation is stated as a problem of regularized clustering, leading to a fully global curve evolution method which we implement via level sets and demonstrate on vector-valued image partitioning. From the viewpoint of regularized clustering, segmentation into a fixed but arbitrary number  $N$  of regions is stated as the simultaneous minimization of  $N - 1$  energy functionals, each involving a single region and its complement. The resulting Euler-Lagrange curve evolution equations yield a partition at convergence provided the curves are initialized so as to define an arbitrary partition of the image domain. We show results on synthetic and natural vectorial images.

## 2. PROPOSED APPROACH

Let  $\mathbf{I} : \Omega \rightarrow \mathbb{R}^n$  be an image defined on  $\Omega \subset \mathbb{R}^2$ . Segmentation consists in determining a partition  $\mathcal{R} = \{\{\mathbf{R}_i\}_{i \in [1, N]}, \mathbf{R}_i \subset \Omega\}$  of  $N$  subsets of  $\Omega$  such that the restriction of the image function to each region best fits a given description, usually given through statistical models.

The problem is commonly stated as the minimization of a functional containing two characteristic terms: a term of conformity to data and a regularization term. Let  $e_i(\mathbf{x})$  be the function that measures conformity to data in region  $\mathbf{R}_i$ , and let

$$\mathcal{E}_i = \int_{\mathbf{R}_i} e_i(\mathbf{x}) d\mathbf{x} \quad (1)$$

Let us first look at the problem without spatial regularization. The

---

This work was supported in part by the National Science and Engineering Research Council of Canada under grant OGP 0004234.

problem, then, consists of determining the partition that minimizes the following functional:

$$\mathcal{E}_\Omega = \sum_{i=1}^N \mathcal{E}_i \quad (2)$$

Let us rewrite (2) as follows:

$$\mathcal{E}_\Omega = \int_{\mathbf{R}_i} e_i(\mathbf{x}) d\mathbf{x} + \sum_{\substack{j=1 \\ j \neq i}}^N \int_{\mathbf{R}_j} e_j(\mathbf{x}) d\mathbf{x} \quad (3)$$

and note the following inequalities on the second term of the right hand side of (2):

$$\begin{aligned} \sum_{\substack{j=1 \\ j \neq i}}^N \int_{\mathbf{R}_j} e_j(\mathbf{x}) d\mathbf{x} &\geq \int_{\mathbf{R}_i^c} \sum_{\substack{j=1 \\ j \neq i}}^N e_j(\mathbf{x}) \chi_j(\mathbf{x}) d\mathbf{x} \\ &\geq \int_{\mathbf{R}_i^c} \min_{j \neq i} (e_j(\mathbf{x})) d\mathbf{x} \end{aligned} \quad (4)$$

where  $\mathbf{R}_i^c$  denotes the complement region of  $\mathbf{R}_i$  and  $\chi_i(\mathbf{x})$  is the characteristic function of region  $\mathbf{R}_i$ .

Because equality occurs in the first line of (4) for a partition, and in the second line for a partition when  $\sum_{j \neq i} e_j(\mathbf{x}) \chi_j(\mathbf{x}) = \min_{j \neq i} (e_j(\mathbf{x}))$ , this leads us to consider the problem from the viewpoint of clustering or quantization [6], and formulate the problem of minimizing (2) as the simultaneous minimization of the following functionals, each corresponding to a two-region problem involving one region and its complement:

$$\xi_i = \int_{\mathbf{R}_i} e_i(\mathbf{x}) d\mathbf{x} + \int_{\mathbf{R}_i^c} \min_{j \neq i} (e_j(\mathbf{x})) d\mathbf{x} \quad i = 1, \dots, N-1 \quad (5)$$

with  $\mathbf{R}_N$  defined by:

$$\mathbf{R}_N = \bigcap_{i=1}^{N-1} \mathbf{R}_i^c \quad (6)$$

One can easily verify that the simultaneous minimization of the  $N-1$  functionals in (5) and convention (6) yield, just as in standard clustering or quantization [6], a partition of the image domain with  $\sum_{j \neq i} e_j(\mathbf{x}) \chi_j(\mathbf{x}) = \min_{j \neq i} (e_j(\mathbf{x}))$ .

However, image data is particular in the sense that it is laid out spatially, and functionals (5) ignore this layout. To account for this spatial layout, we include in (5) a standard regularization term related to the length of region contours. This has the effect of smoothing these contours and removing small region components. Functionals (5) become:

$$\mathcal{E}_\Omega(\mathbf{R}_i|\mathbf{I}) = \int_{\mathbf{R}_i} e_i(\mathbf{x}) d\mathbf{x} + \int_{\mathbf{R}_i^c} \psi_i(\mathbf{x}) d\mathbf{x} + \frac{1}{2} \mathcal{L}(\partial \mathbf{R}_i) \quad (7)$$

where  $\psi_i(\mathbf{x})$  is shorthand for  $\min_{j \neq i} (e_j(\mathbf{x}))$ ,  $\partial \mathbf{R}_i$  denotes the boundary of region  $\mathbf{R}_i$  and  $\mathcal{L}$  is a measure on the length of the boundary. The problem becomes:

$$\begin{cases} \tilde{\mathbf{R}}_i &= \arg \min_{\mathbf{R}_i} (\mathcal{E}_\Omega(\mathbf{R}_i|\mathbf{I})), \quad i \in [1, N-1] \\ \mathbf{R}_N &= \bigcap_{i=1}^{N-1} \tilde{\mathbf{R}}_i^c \end{cases} \quad (8)$$

In the next section we will derive curve evolution equations for the minimization problem (8). We will also show curves evolving according to these equations will not intersect if they do not initially.

### 3. CURVE EVOLUTION EQUATIONS

Let  $\tilde{\gamma}_i : [0, 1] \rightarrow \Omega$ ,  $i = 1, \dots, N-1$  be simple closed planar curves parameterized by arc parameter  $s \in [0, 1]$ . We associate the interior of  $\tilde{\gamma}_i$  to region  $\mathbf{R}_i$ ,  $i = 1, \dots, N-1$ . To obtain the evolution equation of  $\tilde{\gamma}_i$ , we embed the curve in a family of one-parameter curves  $\tilde{\gamma}_i(t) : [0, 1] \times \mathbb{R}^+ \rightarrow \Omega$ . Assuming that functions  $e_i$  of conformity to data are independent of segmentation, and with

$$\mathcal{L}(\tilde{\gamma}_i) = \lambda \oint_{\tilde{\gamma}_i} ds \quad (9)$$

the curve evolution equations for the minimization of  $\mathcal{E}_\Omega(\tilde{\gamma}_i|\mathbf{I})$ ,  $i = 1, \dots, N-1$  are given by the corresponding Euler-Lagrange descent equations. These equations are, where  $\kappa_i$  is the mean curvature function of  $\tilde{\gamma}_i$ , and  $\vec{n}_i$  its outward unit normal function,

$$\frac{d\tilde{\gamma}_i}{dt}(\mathbf{x}) = -(e_i(\mathbf{x}) - \psi_i(\mathbf{x}) + \lambda \kappa_i(\mathbf{x})) \vec{n}_i(\mathbf{x}) \quad (10)$$

These equations are fully global because each involves the region under consideration but the other regions as well.

We will now show that curves evolving according to these equations will not intersect if they do not initially. Let  $\tilde{\gamma}_i$  and  $\tilde{\gamma}_j$  be two distinct curves. If  $\tilde{\gamma}_i$  and  $\tilde{\gamma}_j$  do not intersect initially, they must first meet at a set of points before they can intersect. Velocity of motion of a curve, on the right-hand side of evolution equation (10), has two terms, the curvature term  $(-\lambda \kappa_i \vec{n}_i)$  and the data term  $(d_i(\mathbf{x}) - \psi_i(\mathbf{x})) \vec{n}_i$ . Let us examine the effect of each of the two terms at a point of contact.

#### 3.1. Curvature term

Figures 1 and 2 show the two possible configurations at a point of contact (up to a renaming of the curves). Let  $\mathbf{x}_0$  be the point of contact under consideration.

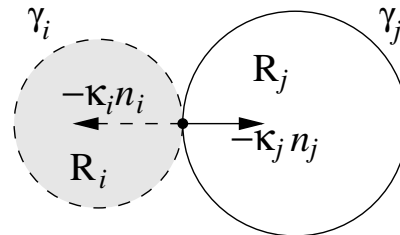


Fig. 1. Case 1

In the first case, both curvatures are positive ( $\kappa_i(\mathbf{x}_0) \geq 0$ ,  $\kappa_j(\mathbf{x}_0) \geq 0$ ). This means that both curves retract and, therefore will not cross at  $\mathbf{x}_0$ .

In the second case, the curvatures are of opposite signs ( $\kappa_i(\mathbf{x}_0) \geq 0$ ,  $\kappa_j(\mathbf{x}_0) \leq 0$ ). This means that the curves move in the same direction. However, because  $|\kappa_i(\mathbf{x}_0)| \geq |\kappa_j(\mathbf{x}_0)|$ , curve  $\tilde{\gamma}_i$  retracts faster than  $\tilde{\gamma}_j$  advances and, therefore the two curves cannot cross at  $\mathbf{x}_0$ .

#### 3.2. Data term

There are two cases to consider:

$$1. e_i(\mathbf{x}_0) = \min_{l \in [1, N]} (e_l(\mathbf{x}_0)) \text{ or } e_j(\mathbf{x}_0) = \min_{l \in [1, N]} (e_l(\mathbf{x}_0)).$$

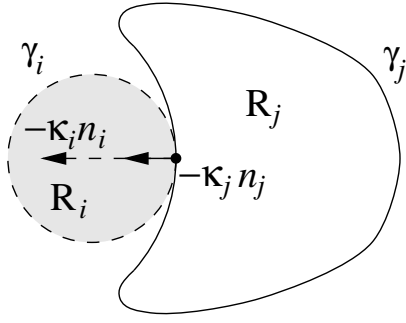


Fig. 2. Case 2

$$2. e_k(\mathbf{x}_0) = \min_{l \in [1, N]} (e_l(\mathbf{x}_0)), \quad k \neq i, k \neq j.$$

In the first case, let us assume, without loss of generality, that  $e_i(\mathbf{x}_0) = \min_{l \in [1, N]} (e_l(\mathbf{x}_0))$ . This means that we have both  $d_i(\mathbf{x}_0) \leq 0$  and  $d_j(\mathbf{x}_0) = e_j(\mathbf{x}_0) - e_i(\mathbf{x}_0) \geq 0$ . Therefore,  $\tilde{\gamma}_i$  and  $\tilde{\gamma}_j$  move in the same direction, with  $\tilde{\gamma}_i$  advancing and  $\tilde{\gamma}_j$  retracting. However, because  $|d_i(\mathbf{x}_0)| \leq |d_j(\mathbf{x}_0)|$ ,  $\tilde{\gamma}_j$  retracts faster than  $\tilde{\gamma}_i$  advances and the two curves will not cross at  $\mathbf{x}_0$ .

In the second case, we have both  $d_i(\mathbf{x}_0) \geq 0$  and  $d_j(\mathbf{x}_0) \geq 0$ . Therefore, the two curves both retract and will not cross at  $\mathbf{x}_0$ , which complete showing that curves moving according to (10) will not intersect if they initially do not.

#### 4. LEVEL SETS IMPLEMENTATION

A level set implementation of curve evolution equations has well known advantageous properties, such as numerical stability and independence to variations of the topology of the curves that can occur during evolution [7]. The idea is to embed curve  $\tilde{\gamma}_i$  as the zero level-set of a function  $\phi_i : \mathbb{R}^2 \rightarrow \mathbb{R}$ , and evolve this function in such a way that its zero level evolves according to Eq. (10). One can easily show [7] that if the evolution of  $\tilde{\gamma}_i$  is described by the equation:

$$\frac{d\tilde{\gamma}_i(s, t)}{dt} = F_i(\tilde{\gamma}_i(s, t), t)\vec{n}_i(s, t) \quad (11)$$

where  $F_i$  is a real-valued function defined on  $\mathbb{R}^2 \times \mathbb{R}^+$ , the evolution equation of function  $\phi_i$ , with the convention that  $\phi_i > 0$  inside the zero level-set, is then:

$$\frac{\partial \phi_i(\mathbf{x}, t)}{\partial t} = F_i(\mathbf{x}, t) \|\vec{\nabla} \phi_i(\mathbf{x}, t)\| \quad (12)$$

In our case, the evolution equation for function  $\phi_i$  is:

$$\frac{\partial \phi_i(\mathbf{x}, t)}{\partial t} = -(e_i(\mathbf{x}) - \psi_i(\mathbf{x}) + \lambda \kappa_i) \|\vec{\nabla} \phi_i(\mathbf{x}, t)\| \quad (13)$$

where the curvature function  $\kappa_i$  is given in terms of the level set function by:

$$\kappa_i = \text{div} \left( \frac{\nabla \phi_i}{|\nabla \phi_i|} \right) \quad (14)$$

To implement the level set equations, one must define extension velocities, i.e., proper velocities at points that do not lie on the evolving curve [7]. For instance, the extension velocity at a point is the velocity at the point closest to it on the evolving curve [8]. Proper extension velocities can also be defined so that the level

set function is at all times the distance function from the evolving curve [7]. Both of these definitions, which are often implemented via narrow banding where the evolution of the level set function is effected only in a neighborhood of the zero level set, require the initial curves intersect the regions they segment. This is important when a region has unconnected components. An alternative robust to initialization, which we use in our experiments, simply extends the expression of velocity on the evolving curve to the image domain, since this expression can be evaluated at every point of the image domain [9, 10, 11]. However, the question arises whether this implementation preserves the property that initially non-intersecting curves evolve without intersection. The property has been observed in our experiments and we are currently working on the question for a formal answer.

Note that the evolution equations (13) reduce to those of other methods, [12] for instance, in the case of a segmentation in two regions. Note also that these equations have been mentioned in [10] as a possible generalization of a two-region motion segmentation formulation.

#### 5. EXPERIMENTAL RESULTS

We validated the algorithm and its implementation in several experiments, two of which we show here. We allow images to be vectorial, and use a Gaussian model for the intensities within regions:

$$e_i(\mathbf{x}) = -\log(p_{\varphi_i}(\mathbf{I})) \quad (15)$$

$$= \frac{n}{2} \log(2\pi) + \frac{1}{2} \log(|\Sigma_i|) + \frac{1}{2} \left( (\mathbf{I}(\mathbf{x}) - \mu_i)^T \Sigma_i^{-1} (\mathbf{I}(\mathbf{x}) - \mu_i) \right) \quad (16)$$

The Euler-Lagrange equations corresponding to the parameters of the Gaussian lead to the following estimates to be computed along with the segmentation [12, 1]:

$$\mu_i^{(l)} = \frac{\int_{\mathbf{R}_i} I^{(l)}(\mathbf{x}) d\mathbf{x}}{\int_{\mathbf{R}_i} d\mathbf{x}}$$

$$\Sigma_i^{(lk)} = \frac{\int_{\mathbf{R}_i} (I^{(l)}(\mathbf{x}) - \mu_i^{(l)}) (I^{(k)}(\mathbf{x}) - \mu_i^{(k)}) d\mathbf{x}}{\int_{\mathbf{R}_i} d\mathbf{x}}$$

where  $l, k \in \{1, \dots, n\}$  and  $n$  is the dimension of the vectorial image.

The image in the first example (Figure 3) is a noisy gray level image with three regions differing in mean gray value<sup>1</sup>. The means are 0, 128 and 256. The noise for the white and grey regions is zero mean Gaussian with standard deviation  $\sigma = 30$ . Noise for the background is Raleigh with  $\sigma = 15$ . The initialization is shown superimposed on the image in Figure 3a. An intermediate step of curve evolution is shown in b), and the segmentation at convergence in c). The three segmented regions represented by their mean gray value is displayed in d).

The image of the second example is a CIElab color image (Figure 4a)<sup>2</sup>. Visual inspection indicates three regions, corresponding to the cat, the car under which, and the ground on which, the cat is laying. Each region exhibits texture and variations in color. The

<sup>1</sup> Courtesy of MGH CMA Internet Brain Segmentation Repository (IBSR)

<sup>2</sup> ©2001 Hoss Firooznia, <http://photoweb.lodestone.org/photo/671/en>

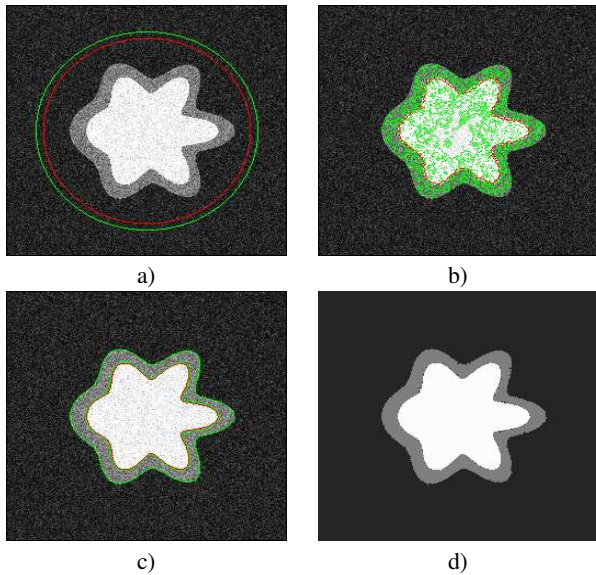


**Fig. 3.** Noisy synthetic image with three regions: a) initialization, b) evolution c) segmentation d) segmented regions with mean grey level value.

results of segmentation are conform to expectation as shown in Figure 4c. The initialization is shown in b) and the three regions of segmentation in d), e), and f).

## 6. CONCLUSION

We examined the problem of image segmentation from the perspective of regularized clustering. This led to a fully global method where segmentation in  $N$  regions is obtained by simultaneous minimization of  $N - 1$  energy functionals describing simpler two-region segmentation problems, each involving a region and its complement. The simple expression of these functionals lends itself to easy derivation of the Euler-Lagrange equations which are implemented via level sets. Experimental results demonstrate the validity of the method.

## 7. REFERENCES

- [1] S. Zhu and A. Yuille, "Region competition: Unifying snakes, region growing, and bayes/MDL for multiband image segmentation," *IEEE Trans. Pattern Anal. Machine Intell.*, vol. 18, no. 9, pp. 884–900, Sept. 1996.
- [2] A. Yezzi, A. Tsai, and A. Willsky, "A fully global approach to image segmentation via coupled curve evolution equations," *J. Vis. Commun. Image Represent.*, vol. 13, no. 1, pp. 195–216, Mar. 2002.
- [3] L. Vese and T. Chan, "A multiphase level set framework for image segmentation using the Mumford and Shah model," *Intern. J. Comput. Vis.*, vol. 50, no. 3, pp. 271–293, 2002.
- [4] N. Paragios and R. Deriche, "Coupled geodesic active regions for image segmentation: A level set approach," in *Proc. European Conf. Computer Vision*, Dublin, Ireland, June 2000, pp. 224–240.

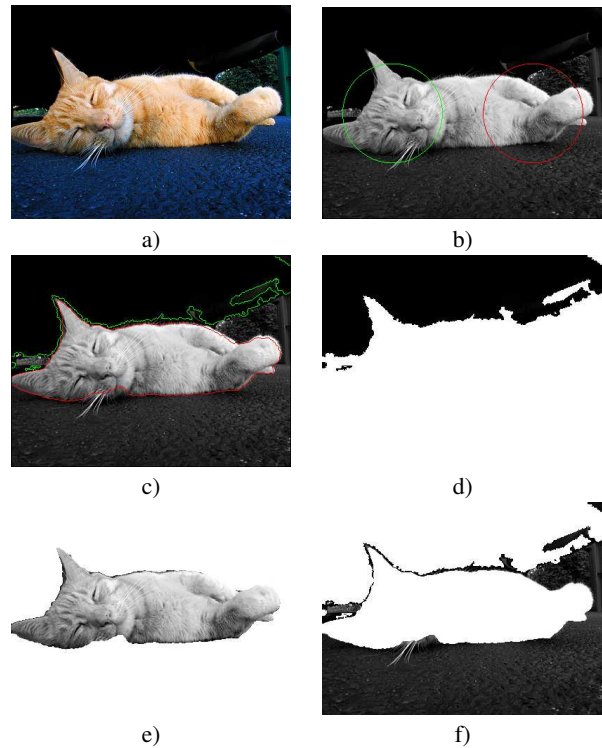


**Fig. 4.** Segmentation of a CIElab color image: a) original, b) initialization, c) computed segmentation, and segmented regions, d) car, e) cat, f) ground

- [5] C. Samson, L. Blanc-Féraud, G. Aubert, and J. Zerubia, "Multiphase evolution and variational image classification," Tech. Rep. 3662, INRIA, Sophia Antipolis Cedex, France, Apr. 1999.
- [6] A. Gersho and R. Gray, *Vector Quantization and Signal Compression*, Kluwer Academic Publishers, 1 edition, 1992.
- [7] J. Sethian, *Level Set Methods and Fast Marching Methods*, Cambridge University Press, 2 edition, 1999.
- [8] R. Malladi, J. Sethian, and B. Vemuri, "Shape modeling with front propagation: A level set approach," *IEEE Trans. Pattern Anal. Machine Intell.*, vol. 17, no. 2, pp. 158–175, 1995.
- [9] C. Rhee, L. Talbot, and J. Sethian, "Dynamical study of a premixed V flame," *Journal of Fluid Mechanics*, , no. 300, pp. 87–115, 1995.
- [10] A.-R. Mansouri and J. Konrad, "Multiple motion segmentation with level sets," *IEEE Trans. Image Processing*, vol. 12, no. 2, pp. 201–220, Feb. 2003.
- [11] A. Mitiche, R. Feghali, and A. Mansouri, "Motion tracking as spatio-temporal motion boundary detection," *Journal of Robotics and Autonomous Systems*, vol. 43, pp. 39–50, 2003.
- [12] M. Rousson and R. Deriche, "A variational framework for active and adaptative segmentation of vector valued images," in *Proc. IEEE Workshop on Motion and Video Computing*, Orlando, FL, Dec. 2002.